Behavioral/Systems/Cognitive

Histamine Influences Body Temperature by Acting at H1 and H3 Receptors on Distinct Populations of Preoptic Neurons

Ebba Gregorsson Lundius, Manuel Sanchez-Alavez, Yasmin Ghochani, Joseph Klaus, and Iustin V. Tabarean
Department of Molecular and Integrative Neurosciences, The Scripps Research Institute, La Jolla, California 92037

The preoptic area/anterior hypothalamus, a region that contains neurons that control thermoregulation, is the main locus at which histamine affects body temperature. Here we report that histamine reduced the spontaneous firing rate of GABAergic preoptic neurons by activating H3 subtype histamine receptors. This effect involved a decrease in the level of phosphorylation of the extracellular signal-regulated kinase and was not dependent on synaptic activity. Furthermore, a population of non-GABAergic neurons was depolarized, and their firing rate was enhanced by histamine acting at H1 subtype receptors. In our experiments, activation of the H1R receptors was linked to the PLC pathway and Ca^{2+} release from intracellular stores. This depolarization persisted in TTX or when fast synaptic potentials were blocked, indicating that it represents a postsynaptic effect. Single-cell reverse transcription-PCR analysis revealed expression of H3 receptors in a population of GABAergic neurons, while H1 receptors were expressed in non-GABAergic cells. Histamine applied in the median preoptic nucleus induced a robust, long-lasting hyperthermia effect that was mimicked by either H1 or H3 histamine receptor subtype-specific agonists. Our data indicate that histamine modulates the core body temperature by acting at two distinct populations of preoptic neurons that express H1 and H3 receptor subtypes, respectively.

Introduction

A role of CNS histamine signaling in thermoregulation has been found in various organisms from invertebrates (Hong et al., 2006) to lower vertebrates (Leger and Mathieson, 1997) and mammals (Green et al., 1976). The neurons of the tuberomammillary nucleus represent the main source of histamine in the brain. They project their axons throughout the brain and control arousal, attention, energy expenditure, feeding, and thermoregulation. Histaminergic fibers are especially dense in the cortex, hypothalamus, amygdala, and striatum (for review, see Haas and Panula, 2003). In the hypothalamus, they are particularly dense in the anterior part (Wada, 1992). The preoptic area/anterior hypothalamus (PO/AH), a region that contains temperature-sensitive neurons and regulates the thermoregulatory "set point," appears to be the main locus in which histamine affects body temperature (Colboc et al., 1982). Histamine injected in the PO/AH induces hyperthermia. Similarly, intra-PO/AH injection of a histamine-*N*-methyltransferase inhibitor, which results in a local increase of histamine concentration, also produces hyperthermia (Gatti and Gertner, 1984). Warm-sensitive neurons in the PO/AH are involved in thermoregulation by sensing local temperature, by integrating peripheral thermal information, and by responding to endogenous pyrogens and cryogens [for review, see Simon (2000) and Boulant (2006)]. However, the neurochemical properties and the local networks formed by preoptic warm-sensitive neurons are not known. Recent studies have revealed that preoptic GABAergic neurons project to and control the activity of thermoregulatory neurons in the rostral raphe pallidus (rRPa) and dorsomedial hypothalamus (DMH) (Morrison et al., 2008).

Histamine actions in the brain are mainly excitatory and involve H1 or H2 subtype receptors. Activation of H1 receptors (H1Rs) results in depolarization and increased firing rate by either the activation of a cationic current (Gorelova and Reiner, 1996; Smith and Armstrong, 1996; Zhou et al., 2006) or by a decrease in a K leak conductance (McCormick and Williamson, 1991; Munakata and Akaike, 1994; Reiner and Kamondi, 1994; Whyment et al., 2006). Similarly, activation of H2 receptors increases excitability by inhibiting K currents (Greene and Haas, 1990; Munakata and Akaike, 1994; Atzori et al., 2000). H3Rs are present at presynaptic terminals and have inhibitory actions on the release of various neurotransmitters in the brain (for review, see Brown et al., 2001). However, postsynaptic inhibitory actions have also been described (Zhou et al., 2006).

An early extracellular study has shown that histamine has mainly excitatory effects on preoptic neurons (Tsai et al., 1989). The cellular and molecular mechanisms underlying these actions

Received Jan. 22, 2010; accepted Feb. 3, 2010.

This work was supported by National Institutes of Health Grant NS060799 (I.V.T.). We thank Prof. Henri Korn (Institut Pasteur, Paris, France) for suggesting a study of histamine effects on preoptic neurons and for comments on an early version of the manuscript. We thank also Prof. Tamas Bartfai (The Scripps Research Institute, La Jolla, CA) for comments and support during the initial period of this study. We thank Dr. Gabor Szabo (The Hungarian Academy of Sciences, Budapest, Hungary) for providing the GAD65-GFP transgenic line. We also acknowledge Brendon Ross for excellent technical support.

Correspondence should be addressed to Iustin Tabarean, Department of Molecular and Integrative Neurosciences, The Scripps Research Institute, 10550 North Torrey Pines Road, SR307, La Jolla, CA 92037. E-mail: tabarean@scripps.edu.

E. G. Lundius's present address: Translational Neuropharmacology L8:01, Karolinska Institute/Center for Molecular Medicine, Karolinska Sjukhuset, 171 76 Stockholm, Sweden.

DOI:10.1523/JNEUROSCI.0378-10.2010

 0270-6474/10/304369-13$15.00/0

are not known. While histamine influences thermoregulation by acting in several hypothalamic regions, we focus in this study on histamine signaling in the median preoptic nucleus (MnPO) because this region appears to be critical in basal thermoregulation as well as in the fever response (Lazarus et al., 2007; Nakamura and Morrison, 2007). Here we study the effects of histamine on identified preoptic GABAergic and non-GABAergic neurons as well as the histamine receptors and signaling pathways involved in these actions to test the hypothesis that the neurotransmitter modulates core body temperature (CBT) by modifying the activity of warm-sensitive preoptic neurons. We also investigate the histamine receptor subtypes involved in the hyperthermic response to histamine.

Materials and Methods

Slice preparation. Coronal tissue slices containing the MnPO were prepared from GAD65-GFP mice (28–42 d old) housed in standard conditions. This transgenic mouse line expresses enhanced green fluorescent protein (eGFP) under the control of the regulatory region of mouse glutamic acid decarboxylase (GAD) 65 gene. The mice were a kind gift from Dr. Gabor Szabo (Hungarian Academy of Sciences, Budapest, Hungary). An animal was anesthetized using isoflurane and killed by decapitation, according to procedures approved by The Scripps Research Institute Animal Welfare Committee. The brain was quickly removed and placed in ice-cold artificial CSF (aCSF) for 2 min. A tissue block containing the hypothalamus was prepared, glued to the stage of a Vibratome 3000 tissue slicer, and placed into the bath of the slicer containing ice-cold oxygenated aCSF. Slices (300 μm thick) were cut and quickly transferred to the recording bath, where they were continuously perfused with oxygenated aCSF and allowed to equilibrate for 2 h at 36–37°C before recording. Patch clamping under visual control was performed with an upright microscope (BX-50, Olympus) equipped with a ×40 water-immersion objective and with fluorescent illumination. We must note that we have selected only brightly fluorescent neurons throughout this study as "GFP positive" and neurons lacking any fluorescence as "GFP negative." Neurons displaying slight fluorescence were not studied. The slice used in our recordings corresponded to the sections located from 0.5 mm to 0.25 mm from bregma in the mouse brain atlas (Paxinos, 2001) to coincide with the cannula location used in our *in vivo* experiments (see below). Recordings were made from neurons in the MnPO and nearby medial preoptic area (MPA) since these regions are not clearly separated in these sections. Although the *in vivo* injections (a volume of 0.2 μl) were directed to the MnPO (see below), some spread to nearby MPA neurons is expected. No differences were noticed between recordings from MnPO and MPA neurons, and thus results were pooled together and the neurons were referred to as "preoptic neurons."

Cell culture. PO/AH cultures were prepared as previously described (Tabarean et al., 2005). The cultures were used at 4–5 weeks after plating. Since at embryonic stage, the preoptic area cannot be distinguished from the anterior hypothalamus, we refer to these cells as "cultured PO/AH neurons."

Patch-clamp recording. The aCSF contained (in mM) the following: 130 NaCl, 3.5 KCl, 1.25 NaH_2PO_4, 24 $NaHCO_3$, 2 $CaCl_2$, 1 $MgSO_4$, and 10 glucose, osmolarity of 300–305 mOsm, equilibrated with 95% O_2 and 5% CO_2, pH 7.4. Other salts and agents were added to this medium. A K^+ pipette solution containing (in mM) 130 K-gluconate, 5 KCl, 10 HEPES, 2 $MgCl_2$, 0.5 EGTA, 2 ATP, and 1 GTP, pH 7.3, was used in most experiments. For recordings of miniature IPSCs, at a holding potential of −10 mV, a Cs pipette solution containing (in mM) 135 Cs-methanesulfonate, 5 CsCl, 10 HEPES, 2 $MgCl_2$, 0.5 EGTA, 2 ATP, and 1 GTP, pH 7.4, was used. For cell-attached recordings, the pipette was filled with aCSF. Glass micropipettes were pulled with a horizontal puller (Sutter Instruments) using Sutter borosilicate glass capillaries with filament. The electrode resistance after back-filling was 2–4 MΩ. No holding current was applied to neurons when recording spontaneous activity in response to temperature changes. All histamine receptor ligands were purchased from Tocris Bioscience, while the other substances were purchased from Sigma. The recording chamber was constantly perfused with aCSF (2–3 ml/min). In electrophysiological experiments, all histamine receptor agonists were applied locally using a perfusion pencil system (tip diameter 100 μm, Automate Scientific) driven by gravity. All the other treatments were bath applied.

Temperature control. The temperature of the external solution was controlled with an HCC-100A heating/cooling bath temperature controller (Dagan) equipped with a Peltier element. To prevent changes induced in the electrode reference potential, the ground electrode was thermally isolated in a separate bath connected to the recording bath by a filter paper bridge.

Data acquisition and analysis. Data were acquired with a MultiClamp 700B amplifier (Molecular Devices) digitized using a Digidata 1320A (Molecular Devices) interface and the Pclamp9.2 software package (Molecular Devices). The sampling rate for the continuous recordings of spontaneous activity was 50 kHz. After establishing whole-cell configuration (or cell-attached), the spontaneous activity of the neuron was recorded for 2–4 min to determine its control behavior at 36–37°C. The spontaneous firing activity of the neurons was recorded in either whole-cell mode (current clamp, $I = 0$) or in cell-attached mode (voltage clamp, $V = 0$). The thermal coefficient of a neuron is defined as the slope of the linear regression fitted to the firing rate versus temperature plot. As in previous reports (Tabarean et al., 2004, 2005), the temperature was varied in the temperature range 34–40°C, and the thermal coefficient was determined over a temperature range of at least 3°C. A neuron having a thermal coefficient higher than 0.8 impulses $\cdot s^{-1} \cdot °C^{-1}$ was defined as warm sensitive. The values of the membrane potential indicated in the figures are those of the potential at the beginning of the illustrated sweeps or, where indicated, of the horizontal reference dotted lines. The input resistance of the neurons was determined as the slope of the fit to the linear region of the *I–V* curve, obtained by injections of hyperpolarizing square current pulses.

Synaptic potentials were detected automatically using the Mini Analysis program (Synaptosoft). The frequency, amplitudes, and kinetics of synaptic events were analyzed using MiniAnalysis software. The statistical significance of differences between cumulative distributions was estimated with the Kolmogorov–Smirnov (K–S) parametric test.

The values reported are presented as mean ± SD. Statistical significance of the results pooled from several cells was assessed with paired *t* test using SigmaPlot software (Systat). Nonparametric one-way ANOVA (Kruskal–Wallis) with Dunn's *post hoc* test ($p < 0.05$) was used for comparison of multiple groups (Prism4, GraphPad Software).

Ca^{2+} imaging. Fura-2 fluorescence signals were acquired with a CCD camera (Hamamatsu ORCA-ER) connected to its frame grabber operating in 8-bit mode and driven by Slidebook software (Intelligent Imaging Innovations). An ultra-high-speed wavelength switcher Lambda DG-4 (Sutter Instruments) equipped with model 340HT15 and 380HT15 filters provided alternating excitation for ratiometric fura-2 measurements. The illumination source was a standard xenon lamp. The sampling frequency of 0.5 Hz was sufficiently fast given the relatively slow responses to histamine or histamine receptor agonists. At this excitation, frequency photobleaching and phototoxicity were minimal. Fura-2 AM (5 mM) was loaded by incubation for 30–60 min at room temperature, in the dark, in 1.5 mM pluronic acid (Invitrogen) in a HEPES-buffered external solution (in mM: 155 NaCl, 3.5 KCl, 2 $CaCl_2$, 1 $MgSO_4$, 10 glucose, and 10 HEPES, pH 7.4). Coverslips containing cell cultures were placed in a laminar flow perfusion chamber (Warner Instrument) and constantly perfused with HEPES-buffered saline (HBS). During Ca^{2+} imaging experiments solutions were exchanged by switching the bath solution. Following subtraction of background fluorescence, the ratio of fluorescence intensity at the two excitation wavelengths was calculated using Slidebook software.

Immunocytochemistry and confocal imaging. Coverslips were washed by immersion in HBS. The H3 agonist *R*-α-methylhistamine (1 μM) or aCSF (control) was applied for 1 min, after which the coverslips were washed in HBS, fixed in ice-cold 4% paraformaldehyde for 30 min, and then incubated for 10 min at room temperature in PBS containing 0.25% Triton X-100. Nonspecific sites were blocked by incubation in PBS con-

Table 1. Primers

Gene	Outer primer pair	Product size (bases)	Inner primer pair	Product size (bases)
GAD65	Fwd: GTGACGAGAGAGAAATG Rev: TGCAGGGTTTGAGATGACCA	784	Fwd: AAGCTGAGTGGAGTAGAGAG Rev: GAGGTACAAACCAGAAGCAG	393
GAD67	Fwd: GATGCCAAACAAAAGGGCTA Rev: GGCTGGGTTAGAGATGACCA	735	Fwd: AAGATGATGGGCGTGCTG Rev: GCTCCAGGCATTTGTTGATCTGGT	244
H1	Fwd: GGACAGACATGGGAAAACTG Rev: TGGGGAGGTAGAAGTTGATG	703	Fwd: GACAAGATGTGTGAGGGGAA Rev: CCATAGAGAGCCAAAAGAGG	286
H2	Fwd: CACTACACCCTCCCAAACTT Rev: ATCCCATCCACCAGTCCATA	664	Fwd: GGCCAAGAAGTGAGTGTAGA Rev: GAAGAGGTTGAGGATGGAAG	366
H3	Fwd: GGACAAGAAGGTAGCCAAGT Rev: AAAGAGTTGAAGGGAGAGGG	798	Fwd: CCGTACACACTCCTCATGAT Rev: CACACTCCAGTTCCACCAAC	403

taining 10% normal goat/horse serum. For double immunostaining, the coverslips were incubated in 2% normal goat serum containing an antibody against phosphorylated CRE-binding protein (pCREB) (1:1000 dilution, Cell Signaling Technology), and antibodies against phosphoextracellular signal-regulated kinase (pERK) (1:400 dilution, Cell Signaling Technology) for 2 h at 37°C. The specificity of the antibodies was checked by the supplier and by previous studies by others. Specific binding was detected by using secondary antibodies conjugated to Alexa Fluor dyes (594, red; 488, green; Invitrogen). Images were collected on a Delta Vision Optical Sectioning Microscope consisting of an Olympus IX-70 microscope. A Photometrics CH 350 cooled CCD camera and a high-precision motorized *x*–*y*–*z* stage were used to acquire multiple consecutive optical sections at a 0.24 μm interval for each of the fluorescent probes by using a 60× oil objective. The settings of the confocal were kept constant so that the images could be analyzed by densitometry and the different conditions could be compared. The experiments were repeated on two different cultures of PO/AH neurons. For cell imaging, 10 different fields in each coverslip were captured, and all neurons in the pictures were analyzed for their green and red fluorescence content. Backgrounds were defined as the fluorescence intensity in non-neuronal fields and subtracted from the values obtained for each neuron. After background subtraction, some neurons displayed little pERK immunofluorescence, while others displayed a very high level of immunofluorescence. In contrast, in the presence of TTX (1 μM), all neurons displayed only a small level of immunofluorescence. Using ImageJ software (NIH), we have quantified the intensity of the fluorescent signal as integrated density for all the neurons studied. The integrated density values for the pERK immunofluorescence in the presence of TTX were similar to the lower ones obtained in normal external solution. The average of the integrated density values in TTX was defined as the "basal" level, and neurons displaying values of at least 50% higher than this level were considered "pERK positive." In contrast, using a similar analysis, we found that PO/AH neurons displayed a wide range of values of pCREB immunofluorescence, which were not affected by TTX.

Cell harvesting and reverse transcription. Cultured PO/AH neurons were patch clamped and then harvested into the patch pipette by applying negative pressure. The content of the pipette was expelled in a PCR tube. First-strand buffer (Invitrogen), 50 ng of random primers (Invitrogen), and H_2O were added to each cell to a volume of 16 μl. The samples were incubated at 65°C for 5 min and then put on ice for 3 min. dNTPs (0.5 mM, Invitrogen), DTT (5 mM, Invitrogen), RNaseOUT (40 U, Invitrogen), and SuperScriptIII (200 U, Invitrogen) were added to each sample to a volume of 20 μl followed by incubation at room temperature for 5 min, at 50°C for 30 min, and then at 70°C for 15 min. After reverse transcription samples were immediately put on ice.

Nested PCR. Gene-specific primers for GAD65, GAD67, H1R, H2R, and H3R were designed using Bisearch (http://bisearch.enzim.hu). All primers are displayed in Table 1. cDNAs were amplified in a volume of 25 μl using a high-fidelity Platinum Taq polymerase kit (Invitrogen) and 0.4 mM dNTPs (Invitrogen). For each gene, 1/10 of the cDNA from each cell was subjected to a first round of PCR using the outer primer pair and a thermal cycling program with an initial denaturation at 94°C for 2 min, 35 cycles of denaturation at 94°C for 15 s, annealing at 55°C for 30 s, and extension at 68°C for 45 s followed by a final extension at 68°C for 10 min.

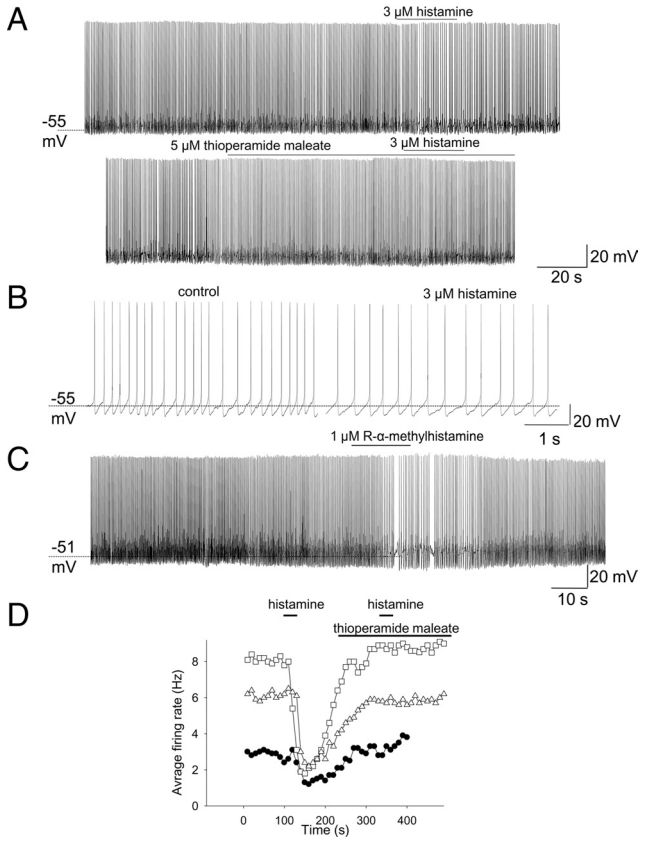

Figure 1. Histamine reduces the firing rate of preoptic GABAergic neurons in slices by acting at H3 subtype receptors. ***A***, Examples of spontaneous firing activity recorded before, during, and after application of histamine (3 μM). The firing rate decreased from 4.1 Hz to 2.2 Hz in response to the neurotransmitter (upper trace). After full recovery of the firing rate, histamine was without effect in the presence of the H3R antagonist thioperamide maleate (5 μM) (lower trace). ***B***, Expanded fragments of the recording in ***A*** showing "pacemaker" firing of the neuron in control (left) and during histamine application (left). ***C***, *R*-α-Methylhistamine (1 μM), an H3R agonist, reduces the spontaneous firing rate of a different preoptic GABAergic neuron. The firing rate averaged 5.3 Hz in the control and 1.9 Hz in the presence of the H3R agonist. ***D***, Average firing rate (for every 10 s) recorded before, during, and after application of histamine (3 μM). After full recovery of the firing rate, histamine was without effect in the presence of the H3R antagonist thioperamide maleate (5 μM). Data are from three neurons. The filled circles (●) correspond to the experiment presented in ***A***. Note that in two neurons, thioperamide caused a slight increase of the firing rate above the control level.

One microliter of the PCR product was subjected to a second round of PCR using the inner primer pair and 40 cycles of the same thermal cycling program as above with the extension time reduced to 30 s. PCR products were visualized by ethidium bromide-stained 2% agarose gel electrophoresis. For each gene, the identity of the PCR product was confirmed by sequencing (The Scripps Research Institute Center for Nucleic Acid

Table 2. Activity of GABAergic and non-GABAergic cells

	GABAergic cells				Non-GABAergic cells			
	Control	H3 ag. (1 μM)	Control	H1 ag. (100 μM)	Control	H3 ag. (1 μM)	Control	H1 ag. (100 μM)
Firing rate (Hz)	7.5 ± 3.1 (5)	2.6 ± 1.9 (5)*	8.1 ± 4.0 (10)	7.9 ± 3.1 (10)	3.1 ± 2.9 (11)	3.2 ± 2.5 (11)	2.9 ± 2.1 (9)	8.3 ± 6.0 (9)*
Input resistance (Ω)	425 ± 105 (10)	433 ± 111 (10)	425 ± 75(10)	415 ± 85 (10)	371 ± 73 (11)	363 ± 76 (11)	359 ± 85 (6)	271 ± 53 (6)*
sIPSC freq. (Hz)	9.6 ± 5.5 (10)	9.2 ± 5.9 (10)	8.3 ± 5.1 (8)	7.9 ± 5.0 (8)	5.8 ± 2.9 (11)	6.2 ± 2.5 (11)	3.9 ± 2.1 (9)	3.8 ± 2.7 (9)
sEPSC freq. (Hz)	10.1 ± 4.8 (10)	9.7 ± 4.9 (10)	9.3 ± 6.1 (8)	8.9 ± 5.5 (8)	11.2 ± 6.9 (11)	11.3 ± 6.9 (11)	10.9 ± 2.1 (5)	21.2 ± 11.2 (5)*
mIPSC freq. (Hz)	3.8 ± 2.1 (6)	3.7 ± 2.0 (6)	4.3 ± 2.8 (5)	4.5 ± 2.7 (5)	4.7 ± 3.1 (5)	4.7 ± 3.1 (5)	4.0 ± 1.9 (5)	3.8 ± 1.7 (5)
mEPSC freq. (Hz)	8.3 ± 3.3 (7)	8.5 ± 3.0 (7)	9.6 ± 2.5 (6)	9.1 ± 2.7 (6)	17.7 ± 14.1 (6)	18.2 ± 15.0 (6)	16.8 ± 11.9 (5)	16.7 ± 12.3 (5)

Values are presented as mean ± SD. *$p < 0.05$. Values in parentheses are numbers of cells. ag., Agonist.

Research) after extraction of the product cDNA from the electrophoresis gel using a QIAquick Gel Extraction Kit (Qiagen).

Radiotelemetry studies of core body temperature and motor activity. Using sterile surgical techniques, an incision was made on the abdomen to separate the skin. The anterior abdominal wall was opened, and the radio transmitter was implanted into the peritoneal cavity. Following appropriate wound closure, the animals were allowed 2 weeks for full recovery before the study. Animal maintenance and experimental procedures are in accordance with the National Institutes of Health *Guide for the Care and Use of Laboratory Animals* (Publication No. 85-23, revised 1985). The telemetry system for monitoring vital signs consists of a surgically implanted radio transmitter (TA10TA-F20, Data Sciences) and a receiver (RPC-1, Data Sciences). CBT and motor activity (MA) sensors were located in the transmitter implant. The cages were positioned onto the receiver plates. Radio signals from the animals' CBT and MA were continuously monitored by a fully automated data acquisition system (Dataquest A.R.T., Data Sciences). C57BL/6 adult males (12–14 weeks old) were used for the *in vivo* experiments.

Stereotaxic injections. Mice were anesthetized (induction 3–5%, maintenance 1–2% isoflurane) via a nose cone and placed into a stereotaxic apparatus. Body temperature was monitored and maintained at 37 ± 0.1°C by a feedback-regulated heating pad. Using sterile surgical techniques, an incision was made to separate the skin. The skull was exposed and three holes were drilled. Two of them were used for screws (diameter 2 mm and length 5 mm) and one of them for the cannula implant (27 ga, 16 mm length). Coordinates for cannula implants in the MnPO were as follows: from bregma: 0.38 mm and ventral 4.6 mm (Paxinos, 2001). After placement, the cannula was secured using dental cement filling out the spaces, including the screws. Following surgery, each mouse was housed in individual Plexiglas recording cages placed in environmentally controlled chambers. The ambient temperature was maintained at ~30 ± 0.5°C in a 12:12 h light–dark cycle-controlled room (lights on 6:00 A.M.). Food and water was available *ad libitum*. Following surgical implantation and appropriate wound closure, the animals were allowed to recover for 2 weeks before the study.

Histamine receptor agonists or the MEK1 inhibitors (U0126 and PD98059) were injected into the MnPO. All substances injected were dissolved in sterile aCSF. Mice were handled for at least 3 d before the injection during 5 min every day for habituation. On the day of injections, mice were held and the injector (cannulae 33 ga, 17 mm length) was placed inside the cannula. The injector was connected to a microsyringe (1.0 μl). The injected volume was 0.2 μl (rate 0.1 μl/min). After this procedure, the animal was returned to the home cage. In some experiments, we first injected aCSF, and after 30 min, we performed a second injection with aCSF or histamine agonist. This sequence allows for a smaller handling-induced hyperthermic spike in response to the second injection and thus allows a better observation of the early phase of the response to histamine agonists. Animals were used for a maximum of two experiments, with an interval of 10 d. Injections were always performed at 10:00 A.M. local time, during the "subjective light period."

Histology. The cannula placement was always checked histologically at the end of the experiments. To this end, blue pontamine dye was injected through the cannulae. The animals were then killed, and the brains were removed and processed for cryosectioning. The placement of the cannula in the MnPO was confirmed for all mice used in this study by visualizing the sections with an inverted microscope.

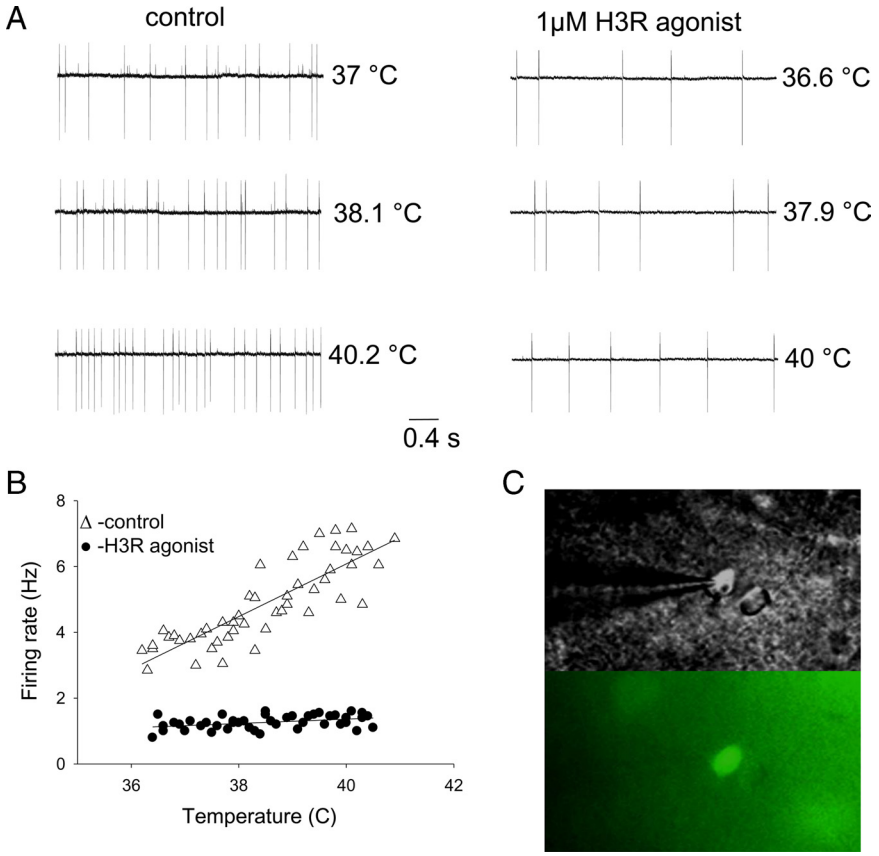

Figure 2. Histamine acting at H3 subtype receptors reduces the firing rate and thermosensitivity of preoptic GABAergic neurons. ***A***, Spontaneous firing activity of a preoptic GABAergic neuron at three different temperatures before (left) and during (right) application of 1 μM *R*-α-methylhistamine. The H3R agonist reduced the firing rate and thermosensitivity of the neuron. The recordings were performed in cell-attached mode. ***B***, Firing rate versus temperature plot. The slope of the linear regression, i.e., the thermal coefficient, decreased from 1.1 impulses · s^{-1} · $°C^{-1}$ to 0.2 impulses · s^{-1} · $°C^{-1}$. ***C***, IR-DIC image (up) and GFP fluorescent signal (down) of the same preoptic GABAergic neuron recorded in a slice from a GAD65-GFP mouse.

Results

Effects of histamine on the spontaneous activity of preoptic GABAergic neurons

Preoptic GABAergic neurons were identified by using the transgenic mouse line GAD65-GFP, which expresses eGFP under the control of the regulatory region of mouse GAD65 gene. Most GABAergic neurons recorded displayed spontaneous "pacemaker" activity (19 of 22), i.e., they presented regular firing patterns and the action potentials were preceded by depolarizing prepotentials (e.g., Fig. 1*B*). The average firing rate of the neurons was 7.5 ± 2.6 Hz ($n = 19$). In 12 of 22 GABAergic neurons studied, histamine (3 μM) applied locally via a perfusion pencil (diameter 100 μm) reduced the spontaneous firing rates by 62 ± 11% ($n = 12$, paired t test $p < 0.05$) (Fig. 1*A*). All neurons inhibited by histamine displayed pacemaker activity (Fig. 1*B*). Higher concentrations of histamine (20 μM) had similar effect, a reduction in firing rate by 66 ± 13% ($n = 4$). This value was not statistically different from the one obtained with 3 μM histamine (ANOVA, $p > 0.1$), suggesting that the effect saturates at low concentrations of the neurotransmitter. The reduction in firing rate by histamine was blocked by the H3R antagonist thioperamide (Fig. 1*A*) in all neurons tested ($n = 5$). Figure 1*D* presents the average firing rate of three neurons in response to histamine, before and after thioperamide incubation. The H3 antagonist appeared to remove an H3R tone in two of six neurons tested: the firing rate increased by 14 ± 5% ($n = 2$) as compared to the initial firing rate of the neuron. The H3R-specific agonist *R*-α-methylhistamine (1 μM) also decreased the firing rate by 64 ± 17% in five of nine GABAergic preoptic neurons tested (Fig. 1*C*). Together with the block by thioperamide, these results indicated that the histamine-induced reduction in firing of GABAergic preoptic neurons is mediated by activation of the H3Rs.

The effect described above was not associated with any obvious change in the frequency of spontaneous (s) IPSPs or sEPSPs. We further studied possible synaptic effects in 5 GABAergic neurons inhibited by the H3R agonist and in 14 GABAergic neurons that did not respond to it, by recording synaptic events in the absence of action potentials at a −50 mV holding potential. The properties (frequency, amplitude, and kinetics) of sIPSCs and sEPSCs in these neurons were not affected by either histamine ($n = 5$) or the H3 agonist ($n = 5$) (Table 2). The holding current and the input resistance of the neurons were not affected by either histamine or the H3R agonist (Table 2). To further address the possibility of synaptic mechanisms, we also studied the effects of *R*-α-methylhistamine (1 μM) in the absence of fast synaptic events, which were blocked by adding CNQX (20 μM), AP-5 (100 μM), and bicuculline (20 μM) to the extracellular solution. In the presence of the antagonists, all five neurons studied maintained their spontaneous firing and the H3R agonist decreased the spike frequency by 71 ± 22% in three of the five neurons studied, a value that was not statistically different from the one obtained with the H3 agonist alone (ANOVA, $p > 0.1$).

We also tested the response of preoptic GABAergic neurons to the H1R agonist 2-pyridylethylamine (100 μM) and to the H2R-specific agonist dimaprit (10 μM) ($n = 10$ and $n = 9$, respectively). The firing rates, input resistance, and synaptic activity of the neurons tested were not affected. Data are summarized in Table 2.

We then questioned whether the preoptic GABAergic neurons that were inhibited by histamine were thermosensitive. The thermosensitivity of the neurons (see Materials and Methods) was measured before and during incubation with *R*-α-methylhistamine (1 μM) (Fig. 2*A*). We found that out of nine GABAergic neurons studied, four were warm sensitive with an average thermal coefficient of 0.9 ± 0.1 impulses · s^{-1} · $°C^{-1}$ ($n = 4$). Three of them were inhibited by the H3R-specific agonist, and their thermal coefficients decreased to 0.4 ± 0.2 impulses · s^{-1} · $°C^{-1}$ ($p < 0.05$, paired t test). Recordings from one of these neurons are presented in Figure 2. The temperature-insensitive neurons displayed an average thermal coefficient of 0.4 ± 0.3 impulses · s^{-1} · $°C^{-1}$ ($n = 5$). Conversely, the firing rate of only one of the five temperature-insensitive neurons tested was reduced by *R*-α-methylhistamine (1 μM). Its thermosensitivity decreased from 0.4 to 0.3 impulses · s^{-1} · $°C^{-1}$.

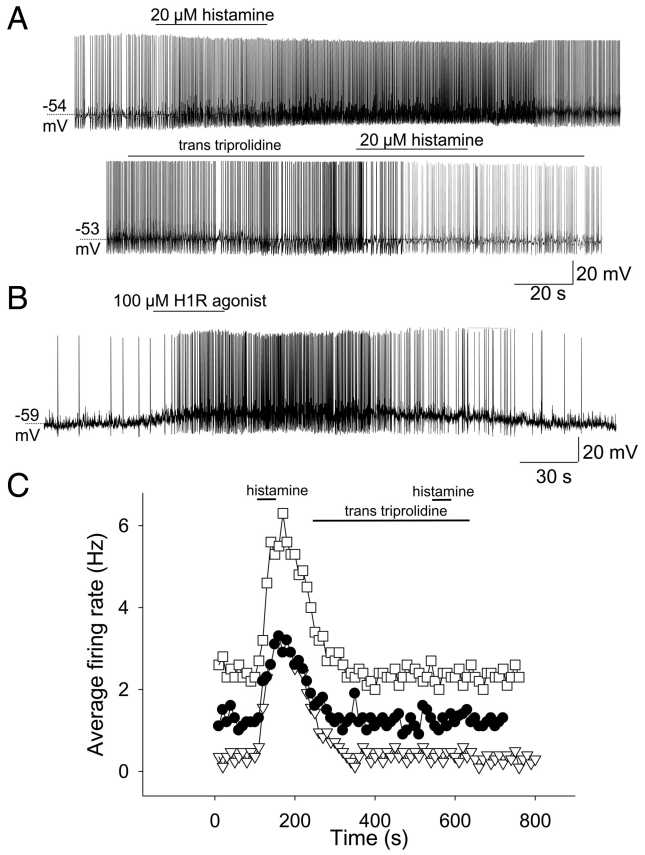

Figure 3. Histamine depolarizes and increases the firing rates of a population of GFP-negative neurons by activating H1 subtype receptors. ***A***, Spontaneous firing activity recorded before (top left) and during (top right) application of histamine (20 μM). Histamine induced a slight depolarization (~5 mV) and increased the firing rate from 1.2 Hz to 3.1 Hz. In the presence of the H1R antagonist *trans*-triprolidine (1 μM) histamine was without effect (lower traces). ***B***, Application of the H1R agonist 2-pyridylethylamine (100 μM) depolarizes and increases the firing rate of a GFP-negative neuron. ***C***, Average firing rate (for every 10 s) recorded before, during, and after application of histamine (20 μM). After full recovery of the firing rate, histamine was without effect in the presence of the H1R antagonist *trans*-triprolidine (1 μM). Data are from three different neurons. The filled circles (●) correspond to the experiment presented in ***A***.

Histamine actions on the spontaneous activity of preoptic non-GABAergic neurons

None of 29 preoptic non-GABAergic (i.e., GFP-negative) neurons studied were inhibited by histamine (3 μM) ($n = 14$) or *R*-α-methylhistamine (1 μM) ($n = 11$); however, a population of GFP-negative neurons (5 of 29) was excited by histamine. The spontaneous firing rates averaged 3.5 ± 2.7 Hz ($n = 5$) and was increased by the neurotransmitter by 94 ± 43% ($n = 5$). This excitation was blocked by the H1R-specific antagonist *trans*-

triprolidine (1 μM) in all neurons tested ($n = 5$) (Fig. 3*A*). The maximal excitatory effect was reached at histamine concentrations of 20 μM or higher. At 20 μM, histamine increased the firing rate by 361 ± 137% ($n = 12$, ANOVA $p < 0.05$) in 12 of 45 neurons tested. The excitatory effect was associated with a depolarization of 2–7 mV (average 3.1 ± 2.0, $n = 12$) in all neurons (Fig. 3*A*). The actions of histamine (20 μM) were blocked by *trans*-triprolidine (1 μM, $n = 3$) or mepyramine (100 nM, $n = 5$). In contrast, the H2R antagonist tiotidine (100 nM) did not affect the histamine effects in all neurons tested ($n = 5$). The H1R agonist 2-pyridylethylamine (100 μM) mimicked these responses: an increase in firing rate by 286 ± 191% ($n = 8$) and a depolarization by 4.0 ± 2.7 ($n = 8$) (Fig. 3*B*). Also the actions of 2-pyridylethylamine (100 μM) were fully blocked by the H1R antagonist mepyramine (100 nM) and were not affected by the H2R antagonist tiotidine (100 nM). At a lower concentration, 2-pyridylethylamine (10 μM) increased the firing rate by 215 ± 89% ($n = 4$). Finally, we also tested betahistine a partial H1R agonist/H3 antagonist that displays little affinity for the H2R (Arrang et al., 1985). Betahistine (100 μM) excited 4 of 15 GFP-negative neurons tested. The betahistine effects were fully blocked by the H1R antagonist mepyramine (100 nM) and were not affected by the H2R antagonist tiotidine (100 nM) (data not shown). Non-GABAergic neurons recorded in voltage-clamp mode displayed an inward current in response to the H1R agonist (Fig. 4*A*), which averaged 21 ± 8 pA ($n = 8$) at −50 mV holding potential. In a subset of these neurons (five of eight), we also noticed an increase in the frequency and amplitude of sEPSCs (Fig. 4*A–C*). The frequency of sEPSCs increased by 94 ± 41% ($n = 5$, paired *t* test, $p < 0.05$) (Table 2), while their average amplitude increased by 105 ± 37% ($n = 5$, paired *t* test, $p < 0.05$). It is interesting to note that in GFP-negative neurons in which H1R agonist did not induce an inward current, we did not find any effects on sEPSCs ($n = 11$). In the presence of TTX, histamine or the H1R agonist induced an inward current (average 16 ± 5 pA, $n = 6$) and decreased the input resistance of the neuron by 24 ± 7% ($n = 6$, paired *t* test, $p < 0.05$) but did not affect the properties of miniature (m)EPSCs in all neurons studied ($n = 6$) (Table 1). Finally, histamine activated an inward current (average 17 ± 7 pA, $n = 3$) when ionotropic glutamate receptors were blocked with CNQX (20 μM) and AP-5 (50 μM). These results indicate that histamine depolarizes non-GABAergic preoptic neurons by a postsynaptic mechanism. Our data also suggest that some H1R-expressing preoptic neurons are glutamatergic and present reciprocal connections and/or present recurrent collaterals.

We also investigated whether the excitatory effects of histamine were present selectively in warm-sensitive or in temperature-insensitive neurons. We found, however, that all non-GABAergic neurons tested were temperature insensitive. Despite the increase in firing rate induced by 2-pyridylethylamine (100 μM) in 5 of 26 neurons studied, the thermal coefficients of the neurons were not significantly affected: their thermosensitivities averaged 0.4 ± 0.3 impulses · s^{-1} · °C^{-1} ($n = 5$) and 0.5 ± 0.2 impulses · s^{-1} · °C^{-1} ($n = 5$) (paired *t* test, $p > 0.1$) in control and during H1R agonist application, respectively. The characteristics of sIPSCs were not affected by the H1R agonist in the GFP-negative neurons studied ($n = 9$) (Table 2).

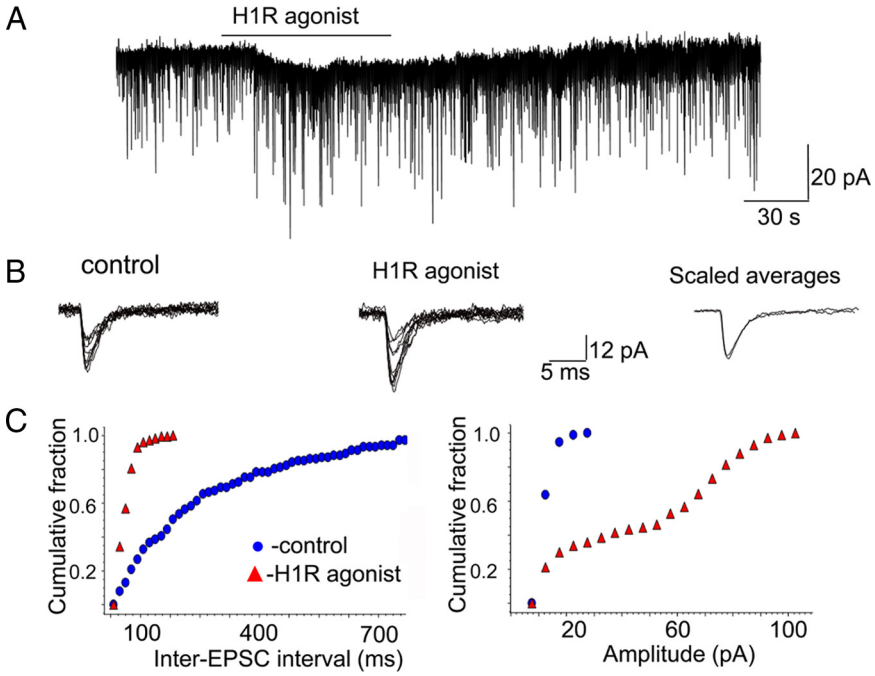

Figure 4. Effects of H1 subtype receptor activation in preoptic GFP-negative neurons. ***A***, Application of the H1R agonist 2-pyridylethylamine (100 μM) results in an inward current and an increase in the frequency of sEPSCs in a GFP-negative neuron. The neuron was voltage clamped at −50 mV. ***B***, Constancy of the sEPSC kinetics. Superimposed, randomly selected sEPSCs ($n = 10$) from the same cell as in ***A***, and their overlapping normalized averages (right traces). ***C***, Cumulative histograms for the inter-EPSCs interval (K–S test $p < 0.01$) and for the amplitudes of the sEPSCs (K–S test, $p < 0.01$) from the same cell as in ***A***.

Finally, the H2R-specific agonists dimaprit (10 μM, $n = 8$) and amthamine (1 μM, $n = 5$ and 10 μM, $n = 5$) were without effect on the membrane potential, firing properties, or synaptic activity of non-GABAergic preoptic neurons.

Lack of effects of the H3R agonist on the spontaneous release of glutamate and GABA

Since H3Rs are present at presynaptic terminals in some central neurons (Garduño-Torres et al., 2007), we have studied the effects of the H3 agonist on the properties of mIPSCs in a group of preoptic neurons. These recordings were performed using the Cs pipette solution at a holding potential of −10 mV as previously described (Tabarean et al., 2006). In either GFP-positive ($n = 6$) or GFP-negative neurons ($n = 5$), the H3R agonist did not affect the characteristics (frequency, amplitude, and kinetics) of the mIPSCs (Table 2). Finally, the H3R agonist did not affect the properties of mEPSCs in any neurons studied ($n = 7$ GFP positive and $n = 6$ GFP negative) (Table 2).

Histamine effects in cultures of PO/AH neurons

We have previously characterized PO/AH neurons in culture and found that they share most properties of PO/AH neurons in slices (Tabarean et al., 2005). Here we have studied the effects of histamine in this culture system and obtained very similar results to those presented above. Briefly, histamine (10 μM) increased the firing rates of PO/AH neurons by 232 ± 110% ($n = 10$), effects accompanied by depolarization (2–5 mV) and/or increased frequencies and amplitudes of sEPSCs in 14% of neurons studied (9

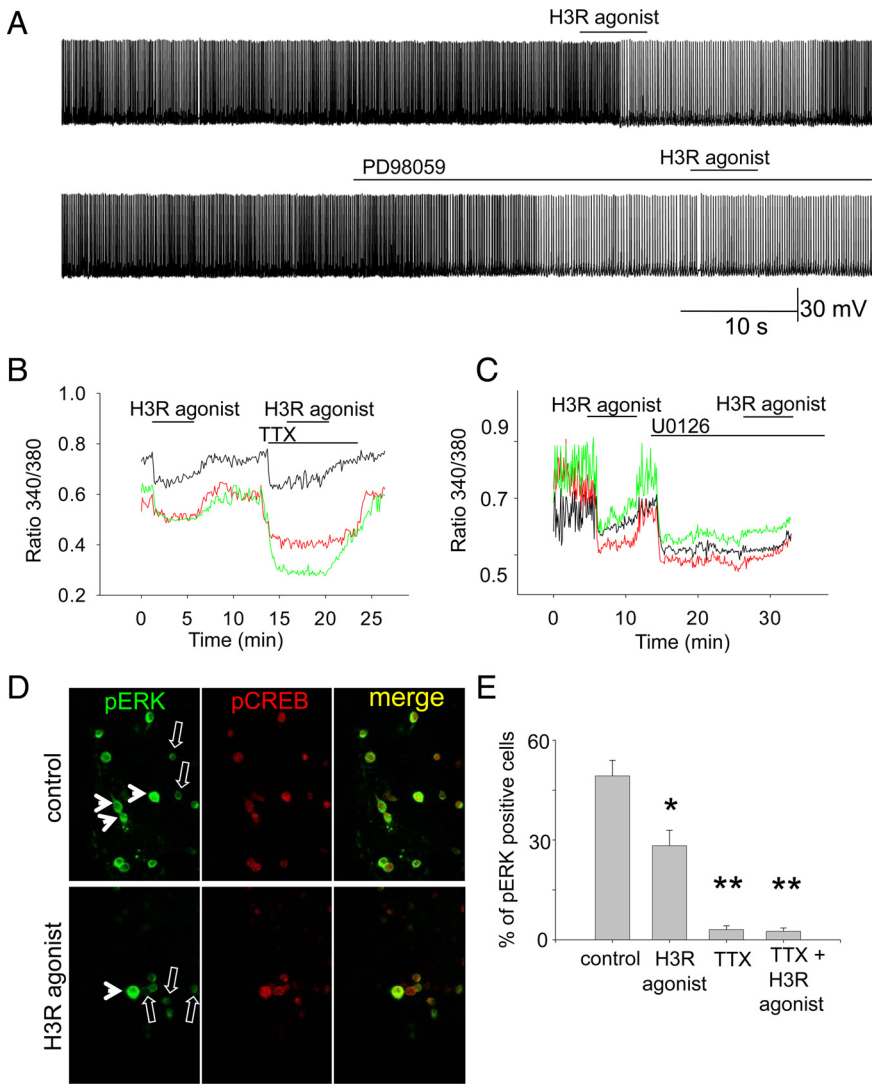

Figure 5. A decrease in the level of phosphorylated ERK accounts for the effects of histamine at H3 subtype receptors. ***A***, Application of the H3R agonist *R*-α-methylhistamine (1 μM) results in a decrease in the spontaneous firing rate in a preoptic GABAergic neuron. After full recovery of the firing rate, treatment with the MEK1/2 antagonist PD98059 (10 μM) also reduces the firing rate of the neuron and occludes any further effect of the agonist (lower trace). ***B***, $[Ca]_i$ responses to *R*-α-methylhistamine (1 μM), TTX (1 μM), and TTX + *R*-α-methylhistamine recorded from three cultured PO/AH neurons. Note that TTX reduces $[Ca]_i$ and occludes the effect of the H3R agonist. ***C***, $[Ca]_i$ responses to *R*-α-methylhistamine (1 μM), the MEK1/2 inhibitor U0126 (10 μM), and TTX + U0126 recorded from three cultured PO/AH neurons. Note that U0126 reduces $[Ca]_i$ and occludes the effect of the H3R agonist. ***D***, Single-channel confocal images showing immunoreactivity to pERK (left, green) and pCREB (middle, red) and their superimposition (right, merge) obtained in control conditions (top) and after 5 min exposure to 1 μM *R*-α-methylhistamine (bottom). Note that some PO/AH neurons present high levels of pERK (arrowheads), while others present low levels of pERK (arrows). ***B–D***, Experiments were performed in bath solutions supplemented with CNQX (20 μM), AP-5 (100 μM), and bicuculline (20 μM) to block fast synaptic transmission. ***E***, Bar chart of the percentage of pERK-positive neurons in control conditions, in the presence of *R*-α-methylhistamine (1 μM), TTX (1 μM), and TTX + *R*-α-methylhistamine. * and ** indicate statistical significance of $p < 0.05$ and $p < 0.01$, respectively (ANOVA followed by Tukey test).

of 62 tested). This action was mimicked by 2-pyridylethylamine (100 μM) and blocked by *trans*-triprolidine (1 μM) in all neurons tested ($n = 8$), suggesting that it was caused by activation of H1Rs. Blocking fast synaptic activity (by adding 20 μM CNQX, 100 μM AP-5, and 20 μM bicuculline to the extracellular solution) did not affect the excitatory action of histamine (10 μM): 3 of 14 neurons tested displayed a depolarization of 2–5 mV and increased their firing rates by 195 ± 85% ($n = 3$).

In a distinct population of cultured PO/AH neurons (11 of 62, ~18%) the firing rate was reduced by histamine (1–10 μM) acting at H3Rs: the effect was mimicked by *R*-α-methylhistamine (1 μM) (data not shown) and blocked by thioperamide. Also this effect of histamine was not dependent on synaptic activity, since it was not affected when fast synaptic activity was blocked. The reduction in firing rate averaged 55 ± 32% ($n = 11$) and 60 ± 25 ($n = 3$) in control and during synaptic block, respectively (ANOVA $p > 0.1$). As was the case in slices, the properties of mIPSCs and mEPSCs were not affected by histamine or by the H1R- or H3R-specific agonist (data not shown). The H3R agonist reduced the frequency of sIPSCs in ~22% (7 of 31) of neurons studied by 46 ± 23% ($n = 7$) (data not shown) and did not affect sEPSCs in the neurons studied ($n = 21$). This discrepancy with the data recorded in slices may be due to different networking: in slices, the H3R-expressing GABAergic neurons may send few local projections, while in dissociated cultures, all projections are "local."

Finally, the H2R-specific agonists dimaprit (10 μM, $n = 12$) and amthamine (1 μM, $n = 6$ and 10 μM, $n = 8$) were without effect on the membrane potential, firing properties, or synaptic activity of PO/AH neurons. Thus, it appears that the postsynaptic responses to histamine in the two preparations were very similar, and consequently we used the cell culture preparation for $[Ca]_i$ imaging and immunocytochemistry experiments aimed at understanding the signaling pathways involved in the histamine actions.

Signaling pathways activated by H1Rs and H3Rs in preoptic neurons

In previous studies, H3R signaling involved either PKA, the extracellular-regulated MAP kinase (ERK), or Ca^{2+} release from intracellular stores (Drutel et al., 2001; Chen et al., 2003; Haas and Panula, 2003). To determine which pathway(s) are involved in H3R signaling in PO/AH neurons, we have performed Ca^{2+} imaging experiments, immunocytochemistry for pERK and pCREB (as a measure of the activation of the PKA pathway), and pharmacological experiments to block the phosphorylation of ERK.

We have first investigated whether blocking the phosphorylation of ERK with the MEK1/2 inhibitors U0126 or PD98059 prevents the electrophysiological effects induced by H3R activation. After measuring the initial inhibitory effect of the H3R agonist, we applied a MEK1/2 inhibitor for 3–5 min. We found that the treatment gradually decreased the firing rate of the neuron and occluded the effect of the H3R agonist (Fig. 5*A*). Similar results were obtained in eight other preoptic GABAergic neurons in slices as well as in seven PO/AH cultured neurons. The results with U0126 (20 μM) and PD98059 (10 μM) were very similar and therefore were pooled together. The MEK1/2 inhibitors decreased the firing rate by 71 ± 17% ($n = 9$)

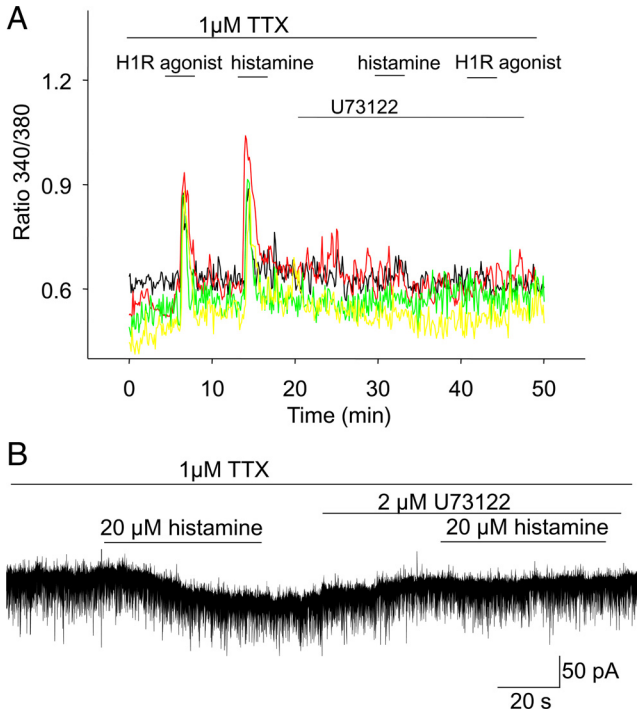

Figure 6. Activation of H1 subtype receptors results in activation of PLC and Ca^{2+} release from intracellular stores. ***A***, $[Ca]_i$ responses to histamine and the H1R agonist 2-pyridylethylamine (100 μM), before and after treatment with the PLC inhibitor U73122 (2 μM) from three cultured PO/AH neurons. Note that U73122 occludes the $[Ca]_i$ responses to histamine and to the H1R agonist. TTX (1 μM) was present in all solutions. ***B***, In the presence of TTX, histamine induces an inward current in a GFP-negative preoptic neuron. The response is abolished by treatment with the PLC inhibitor U73122 (2 μM).

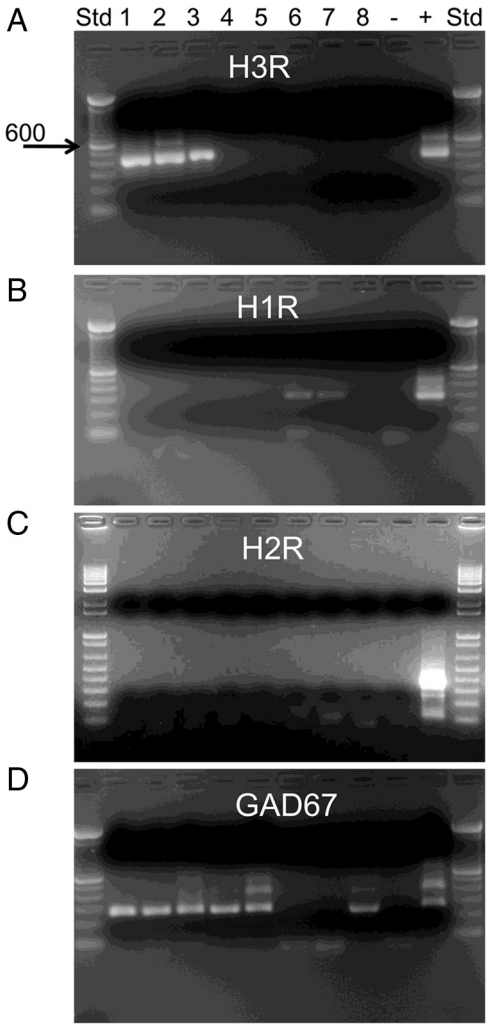

Figure 7. H1R, H2R, H3R, and GAD67 transcripts are present in preoptic neurons in slices. Representative gels illustrating the expression of H3Rs (***A***), H1Rs (***B***), H2R (***C***), and GAD67 (***D***) in eight (1–8) preoptic neurons. The expected sizes of the PCR products are (in base pairs) 403, 286, 366, and 244, respectively. Negative (−) control was amplified from a harvested cell without reverse transcription, and positive control (+) was amplified using 15 ng of hypothalamic mRNA.

in slices and 85 ± 21% ($n = 7$) in cultures. Interestingly, non-GABAergic preoptic neurons were not affected by the two inhibitors ($n = 11$). The responses of non-GABAergic preoptic neurons to the H1 agonist 2-pyridylethylamine (100 μM) were not affected by preincubation with the MEK1/2 inhibitors ($n = 3$, data not shown).

We then examined the effect of histamine on the intracellular Ca^{2+} concentrations $[Ca]_i$ in cultured PO/AH neurons loaded with fura-2 AM. Fast synaptic activity was blocked as above. We found again two patterns of responses in different populations of neurons: in 15% of neurons (49 of 327) histamine induced a robust increase in $[Ca]_i$ (see below), while in 22% of neurons (72 of 327), we saw a clear decrease in $[Ca]_i$. The latter responses were mimicked by the H3R agonist (Fig. 5*B*), while the former were mimicked by the H1R agonist (see below). Interestingly, TTX (1 μM) decreased $[Ca]_i$ to a larger extent in the same neurons and prevented the effect of the H3R agonist (Fig. 5*B*). Similarly, incubation with the MEK1/2 antagonists resulted in a decrease in $[Ca]_i$ and prevented a further decrease in response to the H3R agonist (Fig. 5*C*). The effect of the MEK1/2 antagonists on $[Ca]_i$ was abolished in the presence of TTX (data not shown). These results suggested that activation of H3Rs reduces the firing rate of PO/AH neurons by an ERK-dependent mechanism and that the measured decrease in $[Ca]_i$ reflects less firing activity (and consequently less Ca^{2+} entry through voltage-gated Ca^{2+} channels) rather than an effect on Ca^{2+} stores. Changes in level of pERK and of pCREB in response to H3R agonist incubation (1 μM, 3 min, fast synaptic activity was blocked as above) were measured using immunocytochemistry. We found no evidence for changes in the level of pCREB; however, that of pERK was clearly affected (Fig. 5*D*). In control conditions, 48 ± 8% of neurons ($n = 372$) were pERK positive (see Materials and Methods), while the percentage dropped to 27 ± 6% ($n = 405$) after treatment with H3R agonist (Fig. 5*E*) (ANOVA, $p < 0.05$). Almost no pERK-positive cells could be found in the presence of TTX (3 ± 2%), suggesting that in most PO/AH neurons a high level of pERK reflects firing activity. No effect of the H3R agonist on the level of pERK could be detected in the presence of TTX (Fig. 5*E*).

As mentioned above, histamine induced a robust increase in $[Ca]_i$ in a distinct population of PO/AH neurons. This effect was mimicked by 2-pyridylethylamine (100 μM) (Fig. 6*A*), was blocked by *trans*-triprolidine (1 μM) in 25 of 25 tested neurons (data not shown), and was observed in normal extracellular medium as well as in the presence of TTX (Fig. 6*A*), suggesting that it reflects Ca^{2+} release from intracellular stores, rather than an increase in firing rate. The responses to 2-pyridylethylamine (100 μM) were blocked by mepyramine (100 nM, $n = 15$) and were not affected by the H2R antagonist tiotidine (100 nM, $n = 15$) (data not shown). Betahistine (100 μM) also activated an increase in $[Ca]_i$ that was blocked by mepyramine (100 nM, $n = 11$) and was insensitive to tiotidine (100 nM, $n = 11$) (data not shown).

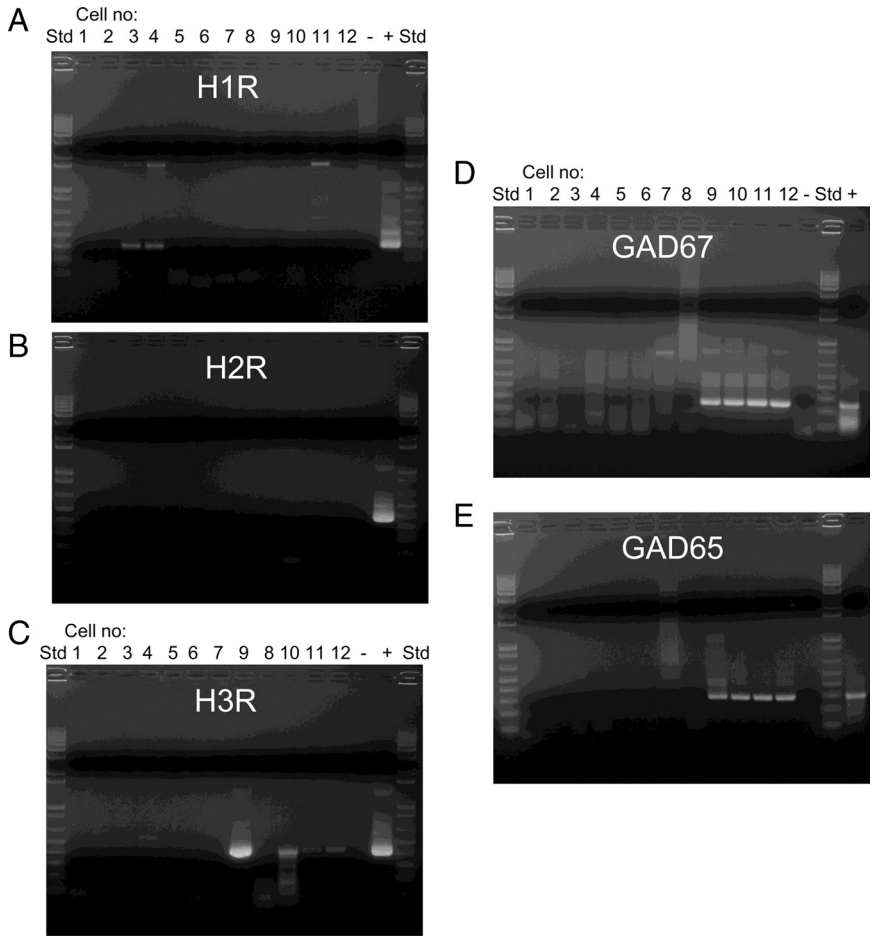

Figure 8. H1R, H2R, H3R, GAD65, and GAD67 transcripts in preoptic neurons recorded in slices from GAD65-GFP transgenic mice. Representative gels illustrating the expression of H1Rs (***A***), H2Rs (***B***), H3R (***C***), GAD67 (***D***), and GAD65 (***E***) in 12 (1–12) preoptic neurons. The expected sizes of the PCR products are (in base pairs) 286, 366, 403, 244, and 393, respectively. Negative (−) control was amplified from a harvested cell without reverse transcription, and positive control (+) was amplified using 15 ng of hypothalamic mRNA. Please note that in ***C***, cells 9 and 8 were loaded in inverse order. Cells 1–8 were GFP negative, while cells 9–12 were GFP positive. Cells 2, 3, and 4 were depolarized by histamine (20 μM), whereas cells 9, 10, 11, and 12 were inhibited by histamine (20 μM). Cells 1, 5, 6, 7, and 8 were not affected by histamine.

Since H1R signaling is usually associated with the PLC pathway (for review, see Haas and Panula, 2003), we have tested the effect of PLC antagonists on the H1R agonist-induced increase in $[Ca]_i$. The $[Ca]_i$ responses were abolished by preincubation with the PLC antagonists U73122 (5 μM) (Fig. 6*A*) or 1-*O*-octadecyl-2-*O*-methyl-*sn*-glycero-3-phosphorylcholine (10 μM) in all cells studied ($n = 157$). Similarly, the H1R agonist-induced inward current was blocked by either of the PLC antagonists (Fig. 6*B*) in all neurons studied in slices ($n = 6$) and in culture ($n = 9$). These results suggest that both the inward currents and the $[Ca]_i$ responses to H1R activation are mediated by the activation of the PLC pathway.

H1 and H3 histamine receptors expression in preoptic neurons

To reveal the cellular distribution of these receptors, we have attempted immunohistochemistry experiments; however, the commercially available antibodies tried by us did not yield specific binding in our preparations. We then performed single-cell reverse transcription-PCR (sc RT/PCR) analysis of the H1, H2, and H3 histamine receptor as well as of the GAD67 mRNA transcripts in 19 preoptic neurons in slices from four different wild-type C57BL/6 mice. Negative (−) control was amplified from a harvested cell without reverse transcription, and positive control (+) was amplified using 15 ng of hypothalamic mRNA. Other controls, including samples of the pipette and bath solutions, were negative after RT-PCR (data not shown). As shown in Figure 7, H1 and H3 receptors were expressed in different subpopulations of preoptic neurons from slices. The H2R could not be detected in any of the 19 neurons (Fig. 7*C*). Out of the 19 preoptic, 9 neurons were GAD67 positive (47%), 4 were H3 positive (21%), and 2 neurons were H1 positive (10%).

We then performed similar experiments in 21 preoptic neurons in slices from GAD65 GFP mice. In this set of neurons, we have characterized the electrophysiological responses to histamine (20 μM) before harvesting the cytoplasm in the patch pipette. In these cells, we also analyzed the presence of GAD65 transcripts. Cells 1–9 and 16–21 were GFP negative, and among them cells 3, 4, and 5 were depolarized by histamine (20 μM), while the rest were not affected. Cells 9–16 and were GFP positive. Histamine (20 μM) decreased the spontaneous firing rate in cells 9–12 and was without effect in the rest. The sc RT/PCR analysis revealed again that H1 and H3 receptors were expressed in distinct sets of neurons and that the excitatory effects of histamine were present in H1-positive neurons (cells 3 and 4, i.e., in two of three cells), while the inhibitory effects of the neurotransmitter were associated with the presence of the H3R (cells 9–12, i.e., four of four cells) (Fig. 8*A*,*B*). The H3R was expressed only in four GFP-positive cells, while the H1R was present in two GFP-negative cells (Fig. 8*A*,*B*). GFP-positive neurons expressed GAD 65 (eight of eight) as well as GAD 67 (seven of eight) (Fig. 8*D*,*E*). GAD65 was absent in all 13 GFP-negative neurons, while GAD 67 was detected in one GFP-negative neuron (data not shown). All H1-positive neurons were GAD65 and GAD 67 negative (two of two), while all the H3-positive neurons expressed both GAD65 and GAD67 (four of four). H2R was not detected in any of the 21 recorded preoptic neurons (Fig. 8*C*). Since previous reports suggested the presence of H2R binding sites and transcripts in the PO/AH (Ruat et al., 1990; Vizuete et al., 1997), we have been surprised by their absence in our studies and performed some additional positive controls. Using the same experimental conditions and primers, we have been able to detect H2R transcripts in granule cells of the dentate gyrus (two of five cells) and dorsomedial hypothalamus (one of three cells) (Fig. 9). Nevertheless we cannot rule out the expression of low levels of the H2R transcripts in preoptic neurons that are not detectable by sc RT/PCR, or their presence in only a very small proportion of neurons.

We also studied the presence of transcripts of the five genes in a set of 10 cultured PO/AH neurons after recording their re-

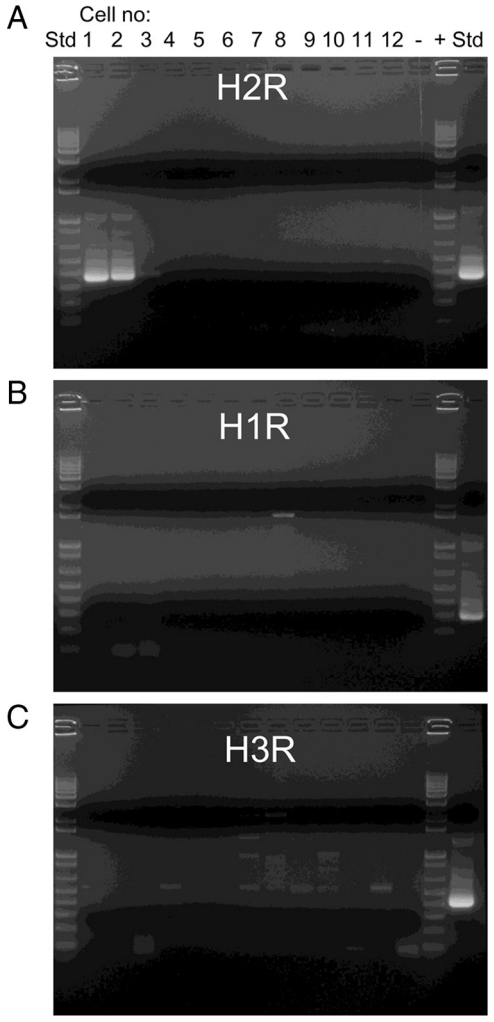

Figure 9. H1R, H2R, and H3R transcripts in hippocampal, DMH, and preoptic neurons in slices from GAD65-GFP mice. ***A–C***, Representative gels illustrating the expression of H2Rs (***A***), H1Rs (***B***), and H2R (***C***) in two granule neurons from the dentate gyrus (1–2), three DMH neurons (3–5), and seven preoptic neurons (6–12). All neurons were GFP negative. The expected sizes of the PCR products are (in base pairs) 366, 286, and 403, respectively. Negative (−) control was amplified from a harvested cell without reverse transcription, and positive control (+) was amplified using 15 ng of hypothalamic mRNA.

sponses to histamine (20 μM). In two (of two) neurons excited by histamine, we have detected H1Rs and none of the other four genes. In two (of two) neurons inhibited by histamine (20 μM), we have detected H3Rs, GAD65, and GAD67 but not H1R or H2R. Out of six neurons not affected by histamine, none expressed H1R, H2R, or H3R, two expressed both GAD65 and GAD67, one neuron expressed GAD65 only, while the remaining three did not present transcripts of either isoform.

Effects of intra-MnPO injection of histamine, H1R agonist, and H3R agonist on core body temperature and motor activity

To assess the effect of histamine on CBT and MA, histamine (10 or 30 μM) or aCSF (control) was injected in the MnPO via a cannula (see Materials and Methods). Experiments were performed in parallel in three groups of six mice. The neurotransmitter induced a dose-dependent hyperthermia when injected in the MnPO (Fig. 10*A*, top), an effect that was not accompanied by increased motor activity (Fig. 10*A*, bottom), suggesting that it was due to changes in thermoregulation (e.g., brown adipose tissue thermogenesis). Within 1 h of the injection (0.2 μl) of 10 or 30 μM histamine, the CBT started to increase and reached a maximum after ~2.5 h. In contrast, aCSF injections (0.2 μl, control) did not result in hyperthermia. The responses to histamine were statistically different from the control (ANOVA, $p < 0.05$ and $p < 0.01$ for the two doses of histamine, respectively).

To determine the receptor subtypes involved, we then injected histamine receptor subtype-specific agonists. The H3R agonist (10 μM, 0.2 μl) induced a rapid increase in body temperature that was almost identical to that induced by histamine (30 μM) with no effect in MA (Fig. 10*B*). The response to H3R agonist was not statistically different from that induced by histamine (30 μM) (ANOVA, $p > 0.1$). Since inhibition of ERK phosphorylation mimicked the effects of H3R agonist in our *in vitro* experiments, we also injected the MEK-1 inhibitors PD98059 (20 μM, 0.2 μl) or U0126 (30 μM, 0.2 μl) intra-MnPO. PD98059 induced a hyperthermia of similar time course to that of the H3 agonist but of smaller amplitude, with no changes in MA (Fig. 10*B*). Nevertheless, the response was different from the control starting at 1 h after injection and up to 6 h later ($p < 0.05$). Similar results were obtained also with the other MEK-1 inhibitor U0126 (data not shown).

Intra-MnPO injection of H1R agonist (100 μM, 0.2 μl) or aCSF (control) was performed in parallel in two groups of cannulated mice ($n = 6$ each). The agonist induced a persistent hyperthermia (ANOVA, $p < 0.01$ when compared to the aCSF control), which reached a maximum at ~2 h after injection and lasted for at least 8 h (Fig. 10*C*, top). No changes in the MA were induced by the H1R agonist (Fig. 10*C*, bottom).

Discussion

Activation of H1Rs and H3Rs induces opposite effects in distinct populations of preoptic neurons

Previous studies have shown that the preoptic area sends tonic GABAergic inhibition to thermoregulatory centers. Here we report that the majority of identified GABAergic neurons displayed pacemaker activity (86%), in agreement with such a tonic inhibitory output. We also report for the first time that preoptic warm-sensitive neurons or at least a subpopulation are GABAergic. The rate of spontaneous firing of most (55%) preoptic GABAergic neurons decreased in the presence of histamine or of an H3R-selective agonist. These agonists also decreased the thermosensitivity of the neurons, further confirming its plasticity (Tabarean et al., 2004). Since H3Rs are usually present at presynaptic terminals, we were surprised to find that the mechanism of inhibition was postsynaptic; however, postsynaptic H3Rs have been recently found also in substantia nigra GABAergic neurons (Zhou et al., 2006). Activation of H1Rs did not affect the firing rate of identified GABAergic preoptic neurons but depolarized and increased the firing rate of a population (17%) of GFP-negative neurons. The frequencies and amplitudes of sEPSCs increased in some of these neurons. These results suggest that H3Rs are present only on preoptic GABAergic neurons, while H1Rs are present on putative glutamatergic neurons. It is interesting to note that only subpopulations of the GABAergic and non-GABAergic neurons were affected by the H3 and H1 agonists, respectively, suggesting heterogeneity among these neuronal subclasses. $[Ca]_i$ imaging also revealed two types of histamine responses when fast synaptic activity was blocked: in some neurons $[Ca]_i$ increased, a response attributed to activation of H1Rs, while in others $[Ca]_i$ decreased, a response attributed to activation of H3Rs. Together these data suggest that two distinct classes of PO/AH neurons express H3Rs

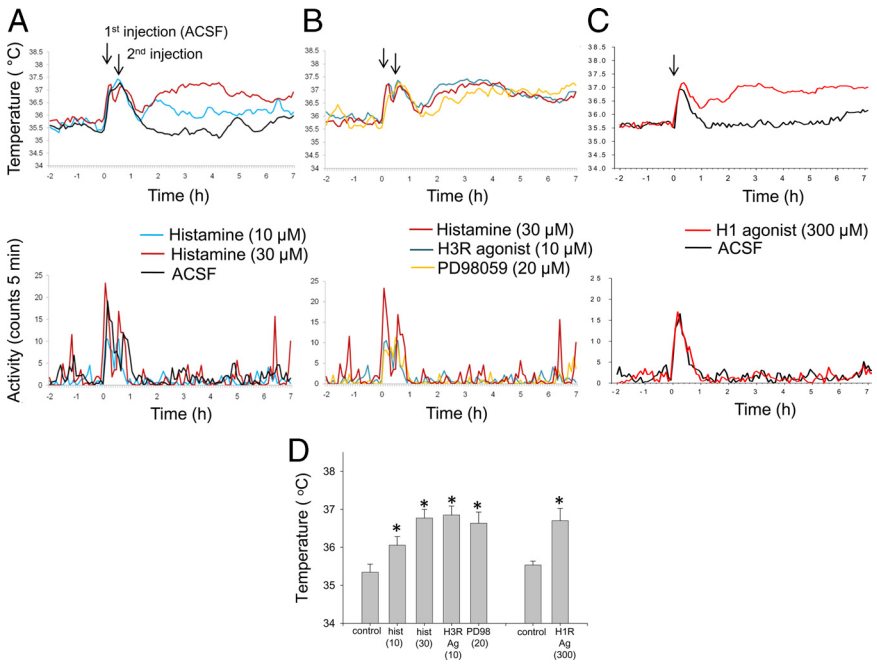

Figure 10. Intra-MnPO injection of histamine receptor agonists induces hyperthermia. ***A***, Intra-MnPO injection histamine produces dose-dependent hyperthermia (top) and does not affect MA (bottom). Responses to injection of 10 and 30 μM histamine (blue and red traces, respectively) and ACSF (control, black trace). ***B***, Intra-MnPO injection of H3 agonist (10 μM) produces hyperthermia (green trace, top) of similar amplitude with the one induced by 30 μM histamine (red trace, redrawn from ***A***) and was without effect on MA (bottom). Injection of PD98059 (20 μM) induces hyperthermia (yellow trace) with no effect on MA. In ***A*** and ***B***, each animal received two injections: all animals received ACSF first. After 30 min, a second injection of ACSF (control) or either histamine (***A***), H3 agonist (***B***), or PD98059 (***B***) was given. This approach decreases the duration of the second stress response and thus the onset of the histamine response can be seen more clearly. ***C***, Body temperature responses to intra-MnPO injection of H1 agonist (300 μM) (orange trace, top) and ACSF (black trace) (top) and the corresponding effect on MA (bottom). ***D***, The histogram provides 4 h (the interval 2–6 h after injection) averages $\pm$ SD at each treatment. (*$p < 0.05$, ANOVA, followed by Tukey test, comparisons were made with the corresponding control injection). ***A–C***, In all experiments the volume injected was 0.2 μl. The line graphs represent averages of data from six mice, through the 7 h recording period. Experiments were performed in parallel in three groups of six mice in ***A*** and ***B*** and in two groups of six mice in ***C***. Note that the trend for an increase in CBT and MA after 6 h corresponds to the circadian rhythm in CBT and MA.

and H1Rs, respectively. Indeed, using single-cell RT/PCR, we found that both in slices and in cultures, H1 and H3 receptors were present in different neurons, the latter being present in GABAergic cells. A similar histamine receptor distribution may be present also in ventromedial hypothalamic nucleus neurons, since the neurotransmitter has opposite effects on the firing rates of populations of neurons (Renaud, 1976).

Signal transduction pathways activated by histamine in preoptic neurons

In PO/AH neurons, activation of H3Rs resulted, surprisingly, in reduced levels of pERK immunoreactivity. We found no evidence of involvement of the PKA pathway or of Ca^{2+} release from intracellular stores. The MEK1/2 antagonists U0126 and PD (which decrease the level of pERK) mimicked the effects of the H3R agonist and occluded the effect of the agonist (or of histamine). In contrast with the result in substantia nigra neurons, we did not record outward currents or hyperpolarization in response to the H3R agonist (Zhou et al., 2006). An alternative mechanism for the decrease in firing rate could be that reduced levels of pERK may result in changes in the phosphorylation state of ion channels involved in "pacemaker" firing activity [e.g., a decrease in the phosphorylation state of Kv4.2 results in increased A-type K currents and consequently in a reduced firing frequency (Yuan et al., 2005)]. Another surprising finding was that in cultured PO/AH neurons, the level of pERK was dependent on neuronal activity and that the H3R agonist was without effect on the pERK level when neuronal activity was blocked. This result raises the possibility that the reduced pERK level reflects a decrease in the firing rate of the neuron and not a direct effect of H3R activation. However, the fact that both MEK1/2 antagonists mimic the effect of the H3R agonist (or histamine) on firing rate and prevent its effect strongly suggests a causal relationship between a decrease in the pERK level and the reduction in firing rate. Together our results indicate that the action of the H3R agonist is activity dependent: potently inhibitory when the neuron is active, and with little effect when the neuron is silent. In agreement with this interpretation was also the finding that no electrophysiological responses to the H3R agonist or to the MEK1/2 antagonists were recorded when neuronal activity was blocked with TTX. $[Ca]_i$ responses mirrored the effects on firing activity: $[Ca]_i$ decreased in response to H3R activation (or to MEK1/2 antagonists) only in the presence of neuronal activity but was not affected in the presence of TTX. These results point to the possibility that the $[Ca]_i$ is a physiological modulator that induces changes in the pERK level as a function of neuronal firing. A similar connection was recently suggested for activity-dependent changes in pERK in DRG neurons (Fukui et al., 2007).

In a distinct set of neurons, H1R activation resulted in Ca^{2+} release from intracellular stores and the activation of an inward current via the PLC pathway. The inward current may be due to activation of Ca-sensitive nonselective cationic channels (Zhou et al., 2006) or to a decrease in a "leak" K conductance (Li and Hatton, 1996; Whyment et al., 2006). The decrease in input resistance in the presence of the H1 agonist suggests that the former possibility is more likely.

We have not detected any H2R activity or H2R transcripts in the preoptic neurons studied here. This finding is in agreement with early studies that suggested the presence of H2Rs in medial or periventricular hypothalamic regions that control heat loss mechanisms, while H1Rs were placed in the rostral hypothalamus (Green et al., 1975; Bugajski and Zacny, 1981).

Implications for putative local networks of preoptic neurons involved in thermoregulation

Little is known about the local neuronal networks comprising preoptic neurons involved in thermoregulation. We found that a population of preoptic GABAergic neurons are inhibited by activation of postsynaptic H3Rs. The H3R agonist did not change the frequency of sIPSCs recorded in preoptic neurons (GFP positive or GFP negative) in slices, which suggests sparse local projections of the H3R-positive GABAergic neurons. In contrast, the fact that the H1R agonist-induced inward current was often accompanied by an increase in the frequency of sEPSCs suggests that the putative H1R-positive glutamatergic neurons form re-

ciprocal connections or present recurring collaterals. We must note that although the agonists were applied locally, it is possible that the cell bodies of nearby neurons were also exposed to them. Thus the changes in sEPSC frequency may be due to activation of H1Rs on either the cell bodies or axons of the presynaptic neuron. On the other hand, the lack of effects of the H1R agonist on the frequency of sEPSCs recorded in GABAergic neurons suggests that putative H1R-positive glutamatergic neurons do not project to nearby GABAergic neurons.

Effect of intra-MnPO histamine on CBT

The hypothalamic concentration of histamine displays a circadian rhythm (Prast et al., 1992) and is dependent on the animal's arousal state, and therefore may be involved in the circadian changes in CBT and/or in those induced by arousal (Valdés et al., 2005, 2006). We report here that intra-MnPO histamine induced a dose-dependent hyperthermia. Activation of either H1Rs or H3Rs in the MnPO resulted in hyperthermia of similar amplitude. An interpretation of our results is that warm-sensitive preoptic GABAergic neurons that express H3Rs contribute to the inhibitory tone sent to neurons in the DMH and/or rRPA that control thermogenesis. Thus, in the presence of histamine, a decrease in the frequency of their tonic firing results in diminished inhibition of downstream thermoregulatory neurons and increased thermogenesis. Our findings may explain the fact that transgenic mice lacking H3Rs display a lower CBT (Takahashi et al., 2002): lack of inhibition by histamine at H3Rs would result in increased activity of preoptic GABAergic neurons that project to rRPA neurons and consequently in decreased thermogenesis.

Interestingly, activation of H1Rs in the MnPO also induced a hyperthermia of similar amplitude to that induced by histamine. Our data *in vitro* showed that activation of H1Rs in preoptic non-GABAergic neurons resulted in increased glutamate release. However, local GABAergic neurons were not affected by it. Indeed, if preoptic GABAergic neurons were excited by H1R activation (directly or via activation of presynaptic neurons), one would expect a decrease in CBT. Together our data strongly suggest that preoptic glutamatergic neurons control at least one thermoregulatory mechanism without having the preoptic GABAergic neurons as intermediate. The wiring of preoptic glutamatergic neurons within thermoregulatory networks is not known. One possibility is the network comprising vasodilator neurons that receive excitatory input from the PO/AH (Nagashima et al., 2000). However, it would be expected that activation of H1Rs in preoptic glutamatergic neurons would result in vasodilation and a decreased CBT, i.e., an effect opposite to that observed. Another possibility is that preoptic glutamatergic neurons project to rRPA neurons controlling thermogenesis directly or via the DMH, in a similar manner to preoptic GABAergic neurons. Such a network may also account for the observation that the maximal hyperthermia reached in response to activation of either H1Rs or H3Rs in the MnPO is similar to that induced by histamine. Either treatment may result in maximal activation of the rRPA neurons; thus, their effects are not additive. The lower affinity of histamine to H1Rs suggests that their activation occurs when the neurotransmitter's concentration is elevated (e.g., during arousal).

References

Arrang JM, Garbarg M, Quach TT, Dam Trung Tuong M, Yeramian E, Schwartz JC (1985) Actions of betahistine at histamine receptors in the brain. Eur J Pharmacol 111:73–84.

Atzori M, Lau D, Tansey EP, Chow A, Ozaita A, Rudy B, McBain CJ (2000) H2 histamine receptor-phosphorylation of Kv3.2 modulates interneuron fast spiking. Nat Neurosci 3:791–798.

Boulant JA (2006) Neuronal basis of Hammel's model for set-point thermoregulation. J Appl Physiol 100:1347–1354.

Brown RE, Stevens DR, Haas HL (2001) The physiology of brain histamine. Prog Neurobiol 63:637–672.

Bugajski J, Zacny E (1981) The role of central histamine H1- and H2-receptors in hypothermia induced by histamine in the rat. Agents Actions 11:442–447.

Chen J, Liu C, Lovenberg TW (2003) Molecular and pharmacological characterization of the mouse histamine H3 receptor. Eur J Pharmacol 467:57–65.

Colboc O, Protais P, Costentin J (1982) Histamine-induced rise in core temperature of chloral-anaesthetized rats: mediation by H2-receptors located in the preopticus area of hypothalamus. Neuropharmacology 21:45–50.

Drutel G, Peitsaro N, Karlstedt K, Wieland K, Smit MJ, Timmerman H, Panula P, Leurs R (2001) Identification of rat H3 receptor isoforms with different brain expression and signaling properties. Mol Pharmacol 59:1–8.

Fukui T, Dai Y, Iwata K, Kamo H, Yamanaka H, Obata K, Kobayashi K, Wang S, Cui X, Yoshiya S, Noguchi K (2007) Frequency-dependent ERK phosphorylation in spinal neurons by electric stimulation of the sciatic nerve and the role in electrophysiological activity. Mol Pain 3:18.

Garduño-Torres B, Treviño M, Gutiérrez R, Arias-Montaño JA (2007) Presynaptic histamine H3 receptors regulate glutamate, but not GABA release in rat thalamus. Neuropharmacology 52:527–535.

Gatti PJ, Gertner SB (1984) The effect of intrahypothalamic injection of homodimaprit on blood pressure. Neuropharmacology 23:663–670.

Gorelova N, Reiner PB (1996) Histamine depolarizes cholinergic septal neurons. J Neurophysiol 75:707–714.

Green MD, Cox B, Lomax P (1975) Histamine H1- and H2-receptors in the central thermoregulatory pathways of the rat. J Neurosci Res 1:353–359.

Green MD, Cox B, Lomax P (1976) Sites and mechanisms of action of histamine in the central thermoregulatory pathways of the rat. Neuropharmacology 15:321–324.

Greene RW, Haas HL (1990) Effects of histamine on dentate granule cells in vitro. Neuroscience 34:299–303.

Haas H, Panula P (2003) The role of histamine and the tuberomamillary nucleus in the nervous system. Nat Rev Neurosci 4:121–130.

Hong ST, Bang S, Paik D, Kang J, Hwang S, Jeon K, Chun B, Hyun S, Lee Y, Kim J (2006) Histamine and its receptors modulate temperature-preference behaviors in *Drosophila*. J Neurosci 26:7245–7256.

Lazarus M, Yoshida K, Coppari R, Bass CE, Mochizuki T, Lowell BB, Saper CB (2007) EP3 prostaglandin receptors in the median preoptic nucleus are critical for fever responses. Nat Neurosci 10:1131–1133.

Leger JP, Mathieson WB (1997) Development of bombesin-like and histamine-like innervation in the bullfrog (*Rana catesbeiana*) central nervous system. Brain Behav Evol 49:63–77.

Li Z, Hatton GI (1996) Histamine-induced prolonged depolarization in rat supraoptic neurons: G-protein-mediated, Ca(2+)-independent suppression of K+ leakage conductance. Neuroscience 70:145–158.

McCormick DA, Williamson A (1991) Modulation of neuronal firing mode in cat and guinea pig LGNd by histamine: possible cellular mechanisms of histaminergic control of arousal. J Neurosci 11:3188–3199.

Morrison SF, Nakamura K, Madden CJ (2008) Central control of thermogenesis in mammals. Exp Physiol 93:773–797.

Munakata M, Akaike N (1994) Regulation of K+ conductance by histamine H1 and H2 receptors in neurones dissociated from rat neostriatum. J Physiol 480:233–245.

Nagashima K, Nakai S, Tanaka M, Kanosue K (2000) Neuronal circuitries involved in thermoregulation. Auton Neurosci 85:18–25.

Nakamura K, Morrison SF (2007) Central efferent pathways mediating skin cooling-evoked sympathetic thermogenesis in brown adipose tissue. Am J Physiol Regul Integr Comp Physiol 292:R127–R136.

Paxinos G, Franklin BJ (2001) The mouse brain in stereotaxic coordinates (2nd Ed.) San Diego: Academic.

Prast H, Dietl H, Philippu A (1992) Pulsatile release of histamine in the hypothalamus of conscious rats. J Auton Nerv Syst 39:105–110.

Reiner PB, Kamondi A (1994) Mechanisms of antihistamine-induced sedation in the human brain: H1 receptor activation reduces a background leakage potassium current. Neuroscience 59:579–588.

Renaud LP (1976) Histamine microiontophoresis on identified hypothalamic neurons: 3 patterns of response in the ventromedial nucleus of the rat. Brain Res 115:339–344.

Ruat M, Traiffort E, Bouthenet ML, Schwartz JC, Hirschfeld J, Buschauer A, Schunack W (1990) Reversible and irreversible labeling and autoradiographic localization of the cerebral histamine H2 receptor using [125I]iodinated probes. Proc Natl Acad Sci U S A 87:1658–1662.

Simon E (2000) The enigma of deep-body thermosensory specificity. Int J Biometeorol 44:105–120.

Smith BN, Armstrong WE (1996) The ionic dependence of the histamine-induced depolarization of vasopressin neurones in the rat supraoptic nucleus. J Physiol 495:465–478.

Tabarean IV, Behrens MM, Bartfai T, Korn H (2004) Prostaglandin E2-increased thermosensitivity of anterior hypothalamic neurons is associated with depressed inhibition. Proc Natl Acad Sci U S A 101:2590–2595.

Tabarean IV, Conti B, Behrens M, Korn H, Bartfai T (2005) Electrophysiological properties and thermosensitivity of mouse preoptic and anterior hypothalamic neurons in culture. Neuroscience 135:433–449.

Tabarean IV, Korn H, Bartfai T (2006) Interleukin-1beta induces hyperpolarization and modulates synaptic inhibition in preoptic and anterior hypothalamic neurons. Neuroscience 141:1685–1695.

Takahashi K, Suwa H, Ishikawa T, Kotani H (2002) Targeted disruption of H3 receptors results in changes in brain histamine tone leading to an obese phenotype. J Clin Invest 110:1791–1799.

Tsai CL, Matsumura K, Nakayama T, Itowi N, Yamatodani A, Wada H (1989) Effects of histamine on thermosensitive neurons in rat preoptic slice preparations. Neurosci Lett 102:297–302.

Valdés JL, Farías P, Ocampo-Garcés A, Cortés N, Serón-Ferré M, Torrealba F (2005) Arousal and differential Fos expression in histaminergic neurons of the ascending arousal system during a feeding-related motivated behaviour. Eur J Neurosci 21:1931–1942.

Valdés JL, Maldonado P, Recabarren M, Fuentes R, Torrealba F (2006) The infralimbic cortical area commands the behavioral and vegetative arousal during appetitive behavior in the rat. Eur J Neurosci 23:1352–1364.

Vizuete ML, Traiffort E, Bouthenet ML, Ruat M, Souil E, Tardivel-Lacombe J, Schwartz JC (1997) Detailed mapping of the histamine H2 receptor and its gene transcripts in guinea-pig brain. Neuroscience 80:321–343.

Wada H (1992) [From biochemistry to pharmacology: the histaminergic neuron system in the brain]. Nippon Yakurigaku Zasshi 99:63–81.

Whyment AD, Blanks AM, Lee K, Renaud LP, Spanswick D (2006) Histamine excites neonatal rat sympathetic preganglionic neurons in vitro via activation of H1 receptors. J Neurophysiol 95:2492–2500.

Yuan W, Burkhalter A, Nerbonne JM (2005) Functional role of the fast transient outward K+ current IA in pyramidal neurons in (rat) primary visual cortex. J Neurosci 25:9185–9194.

Zhou FW, Xu JJ, Zhao Y, LeDoux MS, Zhou FM (2006) Opposite functions of histamine H1 and H2 receptors and H3 receptor in substantia nigra pars reticulata. J Neurophysiol 96:1581–1591.